J Mater Sci (2009) 44:3393–3401
DOI 10.1007/s10853-009-3449-0

Phase separation in immiscible silver–copper alloy thin films

Soumya Nag · Kristopher C. Mahdak · Arun Devaraj · Smita Gohil · Pushan Ayyub · Rajarshi Banerjee

Received: 14 January 2009 / Accepted: 27 March 2009 / Published online: 15 April 2009

Abstract Far from equilibrium, immiscible nanocrystalline Ag–Cu alloy thin films of nominal composition Ag–40 at.% Cu have been deposited by co-sputter deposition. Both X-ray and electron diffraction studies indicate that the as-deposited films largely consist of nanocrystalline grains of a single alloyed face-centered cubic (*fcc*) phase. However, detailed three-dimensional atom probe tomography studies on the same films give direct evidence of a nanoscale phase separation within the columnar grains of the as-deposited Ag–Cu films. Subsequent annealing of these films at 200 °C leads to two effects; a more pronounced nanoscale separation of the Ag and Cu phases, as well as the early stages of recrystallization leading to the breakdown of the columnar grain morphology. Finally, annealing at a higher temperature of 390 °C for a long period of time leads to complete recrystallization, grain coarsening, and a complete phase separation into *fcc* Cu and *fcc* Ag phases.

Introduction

In recent years, there have been a number of studies on far-from equilibrium alloys consisting of thermodynamically immiscible alloying elements. These studies have been well summarized in a recent review [1]. The silver–copper binary system falls in this category with copper and silver being mutually immiscible in the solid state, and exhibits positive enthalpy of mixing in both solid and liquid states [2]. Therefore, based on thermodynamic considerations, solid-state alloying is not permitted at equilibrium, and the mutual solid solubilities of Cu and Ag are typically <0.1% at 300 °C [3]. The large positive enthalpy of mixing for the liquid phase in such systems makes it rather difficult to mix them even in the molten state. Therefore, in many cases, far-from-equilibrium processing techniques, such as vapor deposition and mechanical alloying, have been employed to extend the solid solubility in such systems [4–8]. Since alloy formation is thermodynamically unfavorable in such systems, they exist only in a metastable form, limited by kinetic constraints from phase separating into the equilibrium elemental constituents. Phase separation has also been explored in a number of recent studies reported in the literature, such as in case of Au–Ag core–shell composite films [9], in nanostructured stainless steels [10], as well as by 3D atom probe in bulk nanocrystalline steels [11] and oxide dispersion-strengthened (ODS) alloys [12].

Previous studies on sputter-deposited Ag–Cu alloy films report that depending on the processing conditions, these films either form a supersaturated solid solution [4–6, 13] or a phase-separated mixture of *fcc* Cu-rich and *fcc* Ag-rich solid solutions [13–16]. Deposition of these films on substrates at or above room temperature [13–15], or on negatively biased substrates [16], results in a higher mobility of the vapor atoms on the surface of the growing film leading to phase separation and consequent lowering of the Gibbs free energy. In contrast, if the Ag–Cu films are deposited on liquid nitrogen-cooled substrates, the vapor atoms get rapidly quenched as soon as they arrive at the film surface, and form supersaturated, metastable solid

S. Nag · K. C. Mahdak · A. Devaraj · R. Banerjee (✉)
Center for Advanced Research and Technology and Department of Materials Science and Engineering, University of North Texas, Denton, TX, USA
e-mail: rajarshi.banerjee@unt.edu

S. Gohil · P. Ayyub
Department of Condensed Matter Physics and Materials Science, Tata Institute of Fundamental Research, Mumbai 400005, India

solutions [4–6, 13]. While the results of these studies are interesting, it should be noted that the degree of metastability quenched into these vapor-deposited films, typically determined using standard characterization techniques, would be commensurate with the spatial resolution of the particular technique employed. Thus, for example, the compositional homogeneity of a metastable, supersaturated solid solution in such immiscible systems, as experimentally determined, will be limited by the resolution of the characterization technique. In addition, while the previous studies have focused on the structure and compositional homogeneity of the as-deposited Ag–Cu alloy thin films, there is very limited understanding, if any, on the decomposition of these films during annealing via solid-state phase separation. Therefore, the motivation for this study is twofold:

1. To determine the compositional homogeneity of Ag–Cu alloy thin films, deposited by magnetron co-sputtering on substrates at room temperature, at high spatial resolution using 3D atom probe tomography.
2. To investigate the decomposition route adopted by these films during solid-state phase separation on annealing.

Experimental procedure

The Ag–Cu alloy thin films were deposited using a DC magnetron co-sputtering system. Pure elemental Cu (99.99%) and Ag (99.99%) targets supplied by the Kurt Lesker Company were used for the depositions. The base pressure prior to sputtering was 5×10^{-8} Torr within the deposition chamber, and the pressure of Ar gas maintained during sputtering was 5×10^{-3} Torr. Thin films of composition Ag–40 at.% Cu were deposited with the film thicknesses of $\sim$2 μm. All the films were deposited on Si (100) wafers. For the 3DAP studies, films of the same composition were simultaneously deposited on flat-top silicon microtips. The microtip samples consisted of a 6×6 array of silicon micropillars of dimensions $\sim$5-μm height and $\sim$3-μm flat-plateau diameter on a silicon wafer. Post-thin film deposition by sputtering, the flat-top microtip samples were sharpended to tip radii $\sim$60–70 nm in a dual-beam-focused ion beam (FIB). Further details of the sample preparation procedure have been discussed elsewhere [17]. The as-deposited films were subsequently progressively annealed at 200 °C for 3 h, and, then at 390 °C for 24 h under UHV conditions with the base pressure being 5×10^{-8} Torr. These annealed films were characterized using transmission electron microscopy (TEM), in both plan-view and cross-sectional geometries and three-dimensional atom probe (3DAP) tomography. The TEM studies were carried out in an FEI Tecnai F20 FEG-TEM operating at 200 kV. The 3DAP studies were carried out in an Imago LEAP^{TM} system using the electric-field evaporation mode at a temperature of 70 K, with the evaporation rate maintained at $\sim$0.2% and the pulsing voltage at 20% of the steady-state applied voltage.

Results and discussion

As-deposited Ag–40Cu film

Figure 1 shows the results of TEM analysis of the as-deposited Ag–40Cu thin film in both plan-view and cross-sectional geometries. Figure 1a shows a lower magnification bright-field plan-view TEM image revealing nanometer scale grains viewed normal to the film surface. A selected area electron diffraction (SAD) pattern from this film is shown in Fig. 1b. All the rings in this diffraction pattern can be consistently indexed based on a single *fcc* phase, indicating that this film consists of nanocrystalline grains of a single *fcc* phase, presumably a supersaturated metastable Ag–40Cu solid solution. A higher magnification dark-field plan-view TEM image from the same film is shown in Fig. 1c. Cross-sectional TEM images from the as-deposited film are shown in Fig. 1d–f. From Fig. 1d, it is evident that the grains in this film are columnar in nature with each grain extending over $\sim$100 nm. Therefore, based on the plan-view and cross-sectional TEM images, shown in Fig. 1c and d, respectively, it can be concluded that the as-deposited film consists of columnar grains with diameters ranging from $\sim$10 nm to 40 nm and lengths typically greater than 100 nm. Higher magnification bright-field and dark-field cross-sectional TEM images are shown in Fig. 1e and f, respectively. There appears to be a diffraction contrast in the form of a layered structure visible within individual columns in these higher magnification images. This is more clearly visible in the dark-field image shown in Fig. 1f. While it is rather difficult to speculate regarding the possible origin of this diffraction contrast within the columns based on these images, the possibility of a strain contrast leading to this diffraction contrast cannot be ruled out.

The compositional mapping of the as-deposited Ag–40Cu film was carried out at the nanoscale using 3DAP tomography and the results have been summarized in Figs. 2 and 3. Figure 2a and b show two different perspective views of the same 3D reconstruction of the Cu atoms (in blue) and Ag atoms (in red). The dimensions of this 3D reconstruction are 110 nm × 110 nm × 85 nm. While the viewing direction is nearly perpendicular to the columnar grains in case of Fig. 2a, the viewing direction is parallel to the columns in case of Fig. 2b. Thus the

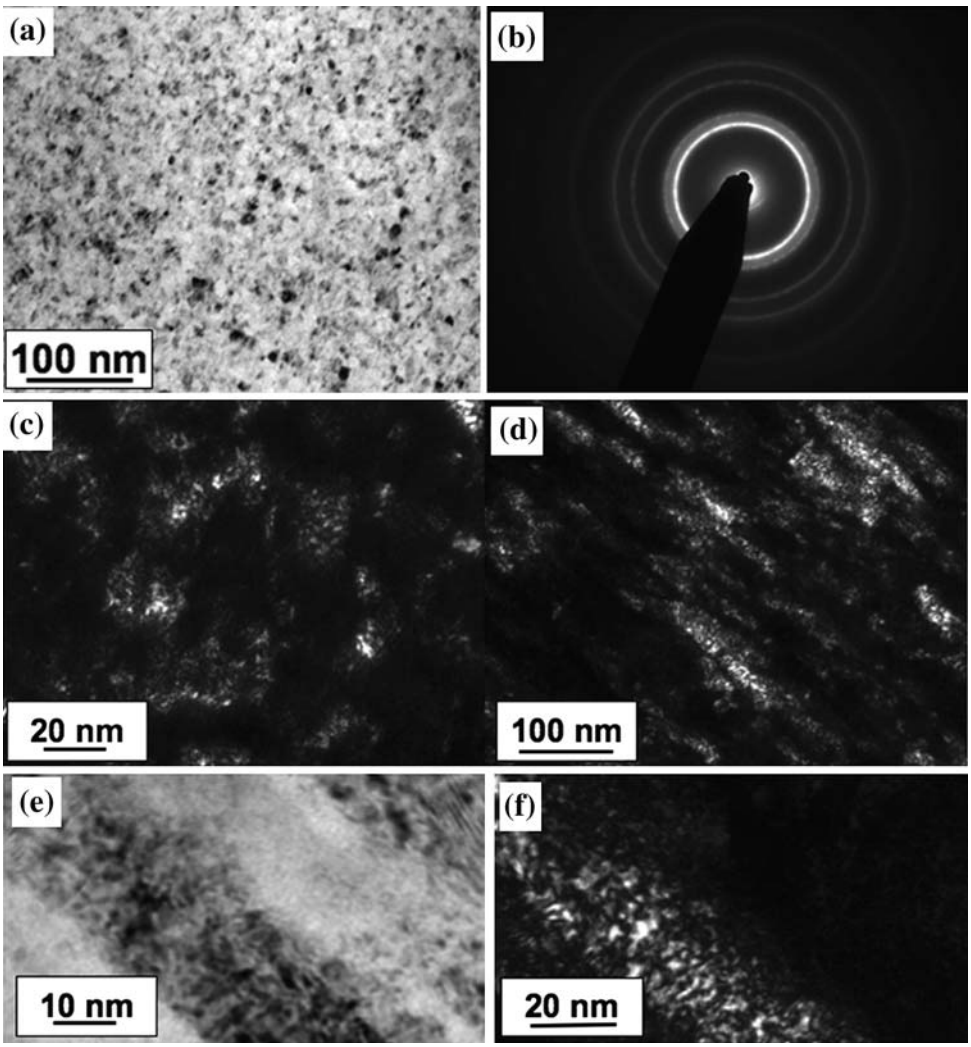

Fig. 1 **a** Low-magnification bright-field plan view TEM image of as-deposited Ag–40Cu thin film showing nanometer scale grains viewed normal to the film surface. **b** Corresponding selected area electron diffraction (SAD) pattern. **c** High magnification dark-field plan-view TEM image from the same film. **d**, **e**, and **f** Cross-sectional TEM images from the same film

inter-columnar boundaries are clearly visible in case of Fig. 2b. The columnar grains are more distinctly visible in the 3D reconstruction shown in Fig. 2c, where the relatively Cu-rich regions have been plotted as an iso-concentration surface (isosurface in short). This isosurface corresponding to 45 at.% Cu, has been plotted in blue, and clearly shows a set of nearly parallel columnar grains. A different perspective view of the 3D isosurface reconstruction is shown in Fig. 2d, where the viewing direction is down the axis of the columns (similar to Fig. 2b). In case of Fig. 2d, the Ag atoms have also been plotted in red. Based on Fig. 2c and d, it is evident that there are two compositionally distinct regions in this microstructure, the columnar grains containing a marginally higher Cu concentration, and the inter-columnar boundary regions containing a relatively lower concentration of Cu. A more detailed analysis of the compositions within the columns as well as in the boundary regions is shown in Fig. 3. Thus, Fig. 3a shows the 3DAP reconstruction in terms of the 45 at.% Cu isosurface together with compositional profiles for both Ag and Cu plotted below the reconstruction. These profiles are plots of the composition versus distance, averaged along a cylinder of diameter 3 nm, with the axis of the cylinder lying parallel to the axis of column, as shown in Fig. 3a. It is evident from these profiles that there are some substantial fluctuations in the Cu concentration within the columnar grain. These fluctuations appear to have a semblance of periodicity, with an average wavelength of $\sim$3.5 nm. The amplitude of these fluctuations could be as large as $\sim$15–20 at.% in some cases. Interestingly, these large-scale compositional fluctuations are not present in the boundary regions between the columnar grains. This is evident from the second set of compositional profiles for Cu and Ag, shown in Fig. 3b. In this case, the profiles have been plotted for a cylinder lying nearly parallel to the axis of the columns, but located in the boundary region between two columnar grains (refer to Fig. 3b). In order to check for the consistency of these observations, the

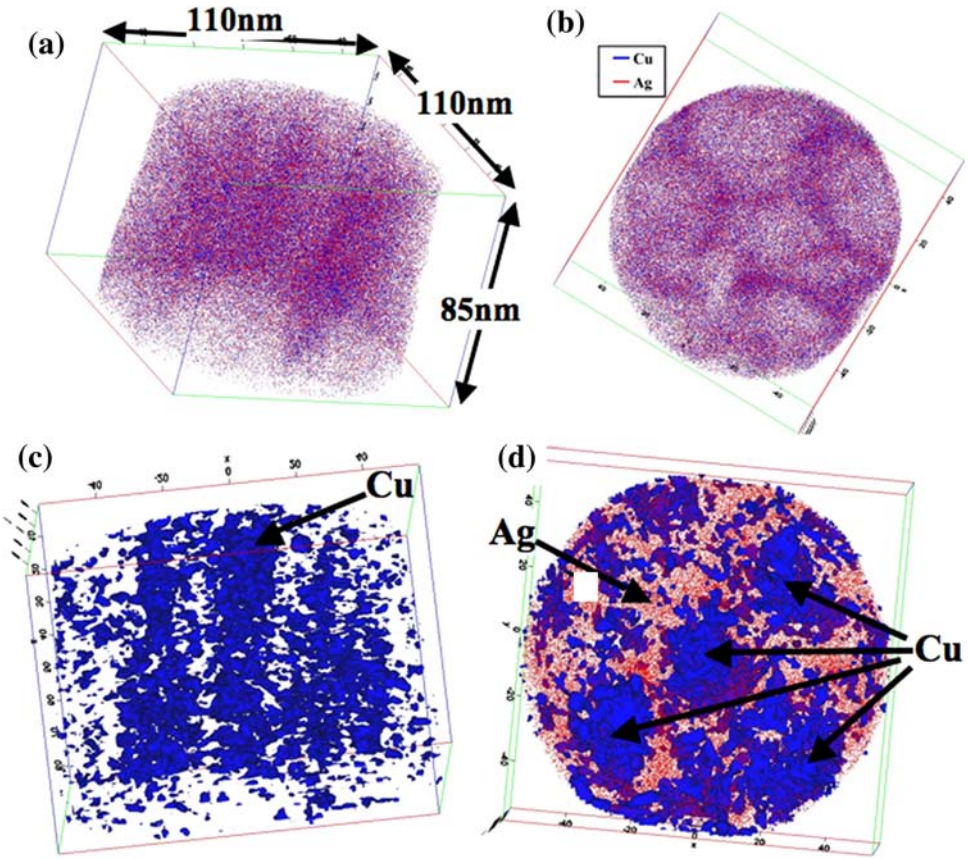

Fig. 2 (Color online) **a** A 110 nm × 110 nm × 85 nm 3DAP reconstruction of as-deposited Ag–40Cu film showing Cu atoms (in blue) and Ag atoms (in red). **b** A different perspective view of the same reconstruction, where the viewing direction is down the axis of the columns. **c** A 45 at.% Cu iso-concentration surface from the same reconstruction showing the Cu-rich regions. **d** A view, similar to that of (**b**), of the same iso-concentration surface superimposed on Ag atoms (in red)

composition profiles were analyzed in a different atom probe specimen made from the same as-deposited Ag–40Cu film, the results shown in Fig. 3c and d. The large-scale compositional fluctuations with an average wavelength of nearly 3.5 nm are clearly visible for profiles constructed along the axis of the columnar grains (Fig. 3c), while these fluctuations are not present in the boundary regions in between the columnar grains, as shown in Fig. 3d.

200 °C/3 h annealed Ag–40Cu film

Annealing the Ag–40Cu film at 200 °C for 3 h led to some major changes in its structure and composition. The TEM results from this 200 °C annealed film are shown in Fig. 4. Figure 4a and c show plan-view and cross-sectional bright-field TEM images, while Fig. 4d shows a cross-sectional TEM dark-field image. From the plan-view bright-field TEM image, shown in Fig. 4a, it appears that the grains in this film have recrystallized to a substantial degree and exhibit much sharper boundaries as compared with the as-deposited microstructure (refer Fig. 1a, c). The cross-sectional image in Fig. 4c shows that the recrystallization process is not yet complete and the semblance of the columnar grains is still visible. In many cases, it appeared that the recrystallized grains nucleated within the parent columnar grains and then grew into adjoining columnar grains, presumably dictated by the misorientation between these columnar grains. However, in some cases the smaller recrystallized grains still lie within a single columnar grain, as shown in the cross-sectional TEM dark-field image in Fig. 4d. In addition, the corresponding electron diffraction pattern from the 200 °C annealed film, shown in Fig. 4b, consists of a larger number of rings as compared with the SAD pattern from the as-deposited film (refer to Fig. 1b). Unlike in case of the as-deposited film, all the rings in the diffraction pattern from the 200 °C annealed film cannot be consistently indexed based on a single *fcc* phase. Rings from two distinct *fcc* phases are clearly visible in this diffraction pattern indicating that the phase separation into two distinct *fcc* phases (rather than a single supersaturated *fcc* phase) with different lattice parameters has been initiated after the 200 °C annealing.

The 3DAP results from the 200 °C-annealed film has been summarized in Fig. 5. The reconstruction in Fig. 5a shows Cu atoms (in blue) and Ag atoms (in red), while the one in Fig. 5b shows the relatively Cu-rich regions in the isosurface representation for 47 at.% Cu, within a 65 nm × 65 nm × 560 nm volume. Large columnar grains,

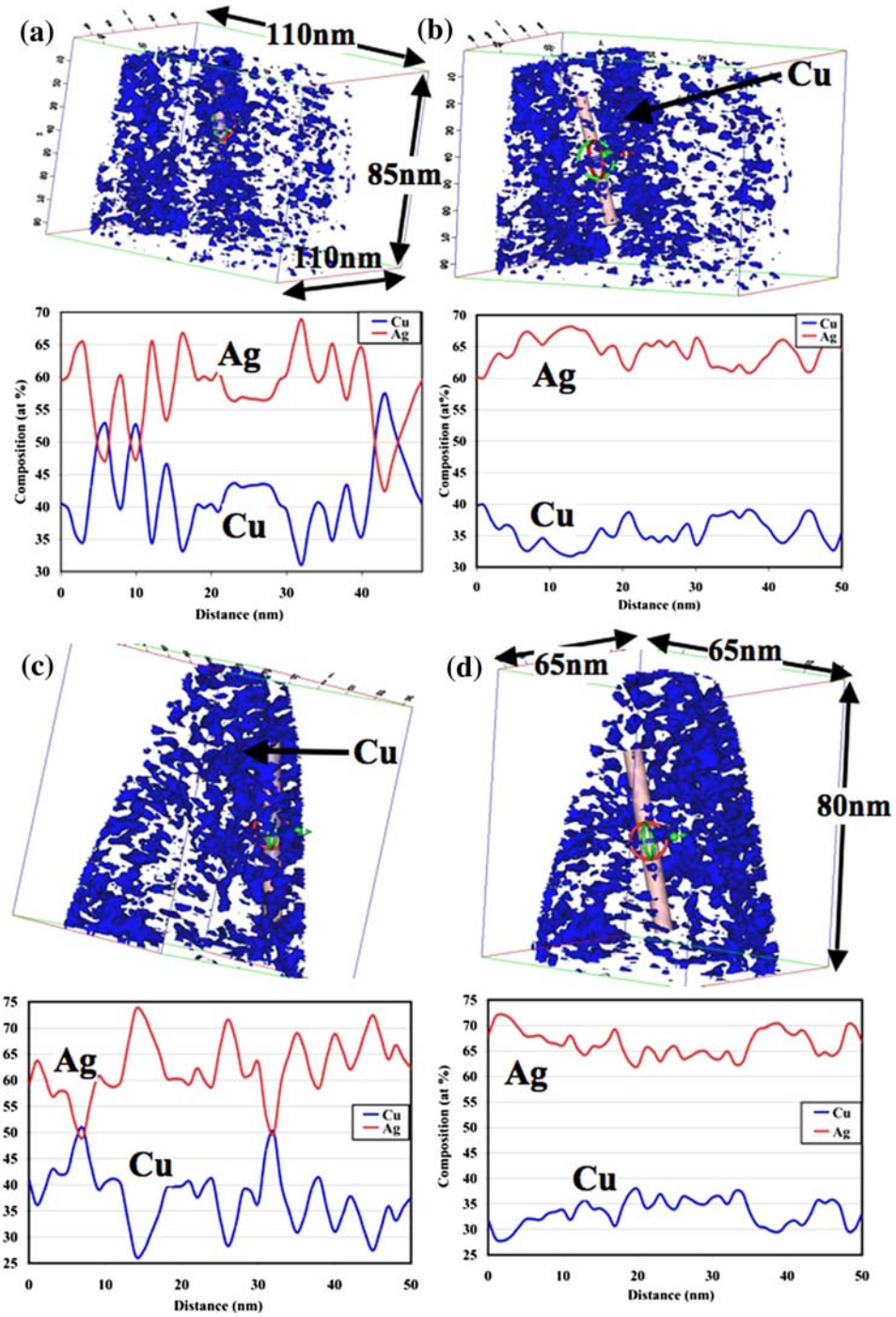

Fig. 3 (Color online) **a** The same 45 at.% Cu iso-concentration surface as in Fig 2 shown along with a compositional cylinder of 3-nm diameter with the axis of the cylinder lying parallel to the axis of column, and corresponding compositional profile. **b** The same iso-concentration surface with the compositional cylinder lying nearly parallel to the axis of the columns, but located in the boundary region between two columnar grains, and corresponding compositional profile. **c** and **d** Similar compositional analyses as in (**a**) and (**b**), respectively, but with a different 45 at.% Cu iso-concentration surface reconstruction of the as-deposited Ag–40Cu film

marginally rich in Cu content, are clearly visible in these atom probe reconstructions. This indicates that the columnar morphology has not been completely destroyed in the 200 °C-annealed film, in agreement with the TEM observations. Magnified views of the Cu-rich regions within this 3DAP reconstruction are shown in Fig. 5c and d. Within a single columnar grain, by using a 47 at.% Cu isosurface view Fig. 5c clearly shows that while certain regions exhibit a pronounced compositional layering, adjacent regions have broken up into smaller Cu-rich grains that exhibit a more equiaxed morphology. These equiaxed Cu-rich grains, shown in greater detail by a 80 at.% Cu isosurface view in Fig. 5d, are presumably formed from the early stages of recrystallization within the previously formed columnar structure, again in agreement with the TEM observations. The recrystallized grains, such as the one marked in Fig. 5d, are of composition 97 at.% Cu–3 at.% Ag, indicating that these recrystallized grains

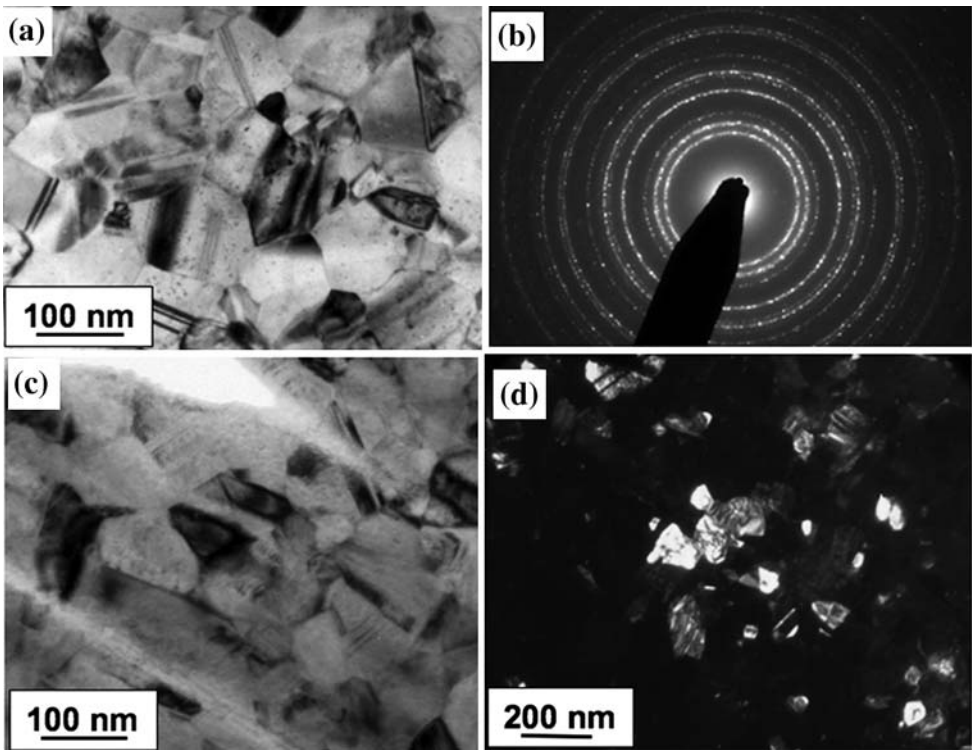

Fig. 4 **a** Plan-view bright-field TEM image of 200 °C/3 h annealed Ag–40Cu film. **b** Corresponding selected area electron diffraction (SAD) pattern. **c** Cross-sectional bright-field TEM image of the same film. **d** Cross-sectional TEM dark-field image of the same film

are close to their thermodynamic equilibrium composition. The regions that have not undergone recrystallization yet, visible in part of the reconstruction shown in Fig. 5c, exhibit a strong nanoscale compositional layering. Compositional profiles across this particular region, averaged across a cylinder of diameter 3 nm (shown in Fig. 5c), have been plotted in Fig. 5e. Interestingly, these compositional modulations exhibit quite a long-range and reproducible periodicity with an average wavelength of ~4 nm. These compositional modulations appear to be a later stage of development of the strong compositional fluctuations visible within the columnar grains in the as-deposited Ag–40Cu thin film (Fig. 3). Interestingly, the average wavelength of the compositional fluctuations in the as-deposited film was also quite similar ~3.5 nm. These results strongly suggest that annealing at 200 °C for 3 h initially leads to a more pronounced development of the nanoscale compositional fluctuations within the columnar grains into longer range periodic modulations, eventually leading to the recrystallization of this nanoscale-layered structure into equiaxed grains of the equilibrium phases of *fcc* Cu and *fcc* Nb. In other words, the 200 °C-annealed film appears to be at an intermediate stage of phase separation into the equilibrium decomposition products.

The nanoscale compositional modulations observed in case of both the as-deposited as well as the 200 °C/3 h annealed Ag–40Cu thin film can possibly be attributed to phase separation via a spinodal decomposition process in these films. As discussed previously, the Ag–Cu system is an immiscible system with a large positive enthalpy of mixing (ΔH_{mix}) of the constituent elements. Such systems with a large ΔH_{mix} typically exhibit a large miscibility gap in the phase diagram within which lies a region of spinodal decomposition. Compositions lying within this region undergo phase separation via a spinodal decomposition process, while those compositions lying in the region between the spinodal and the bimodal (miscibility gap) typically phase separate via a nucleation and growth process. The composition of Ag–40 at.% Cu lies within the spinodal region, and therefore a metastable phase of this composition is expected to undergo phase separation via a spinodal decomposition process. Characteristic features of spinodally decomposed microstructures include nanoscale compositional modulations that typically develop along specific crystallographic directions of the solid matrix phase. These modulations extend within individual grains all the way to the grain boundary. The 3DAP results reported in this article clearly show that the compositional modulations within the columnar grains in the Ag–40Cu thin film extend to the grain boundaries while the boundary regions do not exhibit such modulations. Furthermore, these compositional modulations tend to lie nearly parallel to the axis of the columnar grains, or parallel to the film normal in the most cases. More detailed investigations of the crystallography of these modulations are currently being carried out to determine the details of the nature of spinodal decomposition prevalent in the Ag–40Cu thin films.

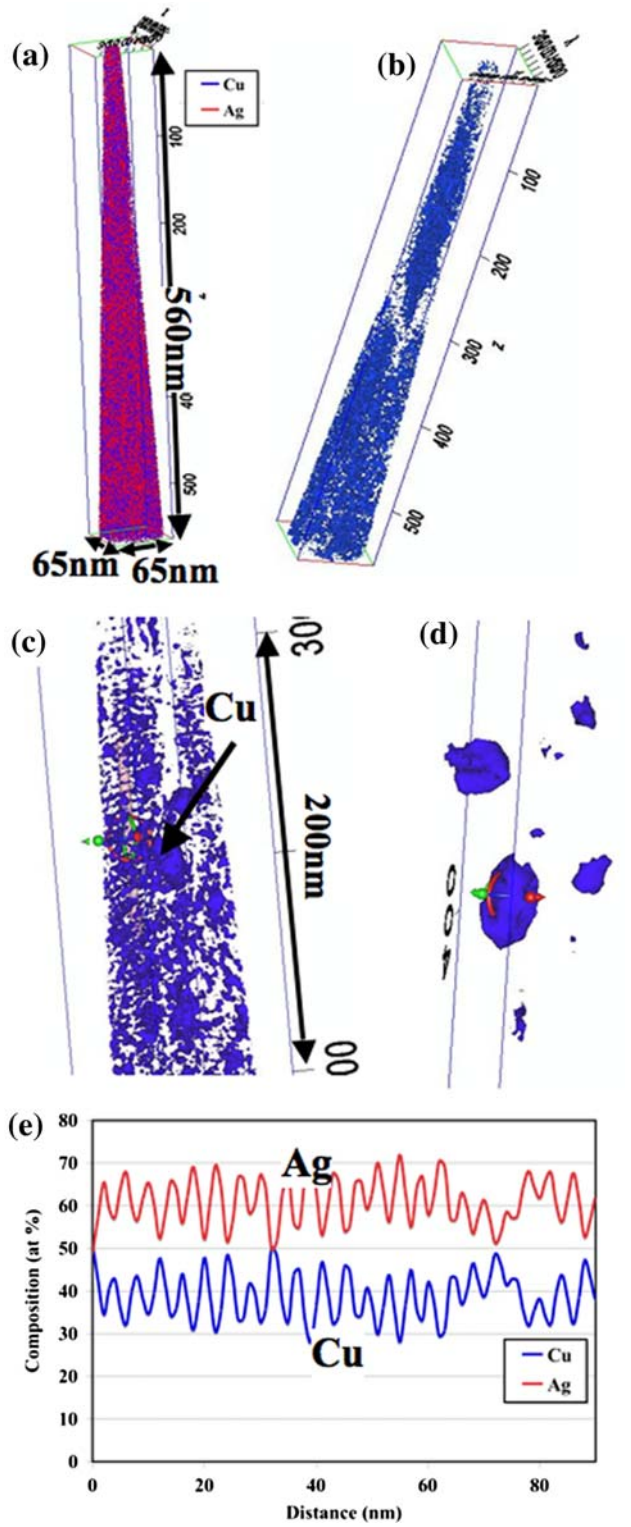

Fig. 5 (Color online) **a** A 65 nm × 65 nm × 560 nm 3DAP reconstruction of 200 °C/3 h annealed Ag–40Cu film showing Cu atoms (in blue) and Ag atoms (in red). **b** A 47 at.% Cu iso-concentration surface from the same reconstruction showing the Cu-rich regions. **c** and **d** Magnified views of the Cu-rich regions within this 3DAP reconstruction. **e** Compositional profile across a region marked in (**c**), averaged across a cylinder of 3-nm diameter

390 °C/24 h annealed Ag–40Cu film

Subsequent to the 200 °C/3 h annealing, in order to drive the phase separation process to completion and achieve the thermodynamic equilibrium phases, the Ag–40Cu film was finally annealed at 390 °C for 24 h. The plan-view bright-field TEM image in Fig. 6a clearly shows relatively large grains exhibiting faults, such as twins, within the grains. The SAD pattern shows distinct rings corresponding to both the *fcc* Cu and *fcc* Ag phases, similar to the case of the 200 °C-annealed film. The 3DAP results from the 390 °C-annealed film have been summarized in Fig. 6c–e. While Fig. 6c shows the Cu (blue) and Ag (red) atoms within a 50 nm × 50 nm × 590 nm volume, Fig. 6d shows a 50 at.% Cu isosurface representation, clearly outlining the Cu-rich regions within this atom probe reconstruction. These regions correspond the recrystallized *fcc* Cu grains. The state of phase separation between the two phases is visible in the compositional profiles for Cu and Ag shown in Fig. 6e. These profiles represent the compositional changes along a 3-nm diameter cylinder, across an interface between an *fcc* Cu grain and an *fcc* Ag grain, as shown in the isosurface representation in Fig. 6e. Note that the cylinder has been aligned nearly perpendicular to the interface at the specific location where it is placed. It is evident from these compositional profiles that the compositional partitioning between Cu and Ag is complete in this condition with the compositions of the Cu and Ag grains being nearly 100 at.% Cu and 100 at.% Ag, respectively. Thus, the annealing at 390 °C for 24 h appears to have completed the phase-separation process into the equilibrium *fcc* Cu and *fcc* Ag phases.

Summary and conclusions

The experimental results obtained from the detailed TEM and 3D atom probe analysis of as-deposited and annealed immiscible Ag–40 at.% Cu alloy thin films can be summarized as follows:

1. The as-deposited Ag–40Cu film primarily exhibits a columnar microstructure. These columnar grains are marginally richer in Cu as compared with the boundary regions in between the columnar grains. The columnar grains consist of a single supersaturated *fcc* solid solution phase and exhibit unidirectional nanoscale compositional fluctuations along the axis of the columns, as revealed by 3DAP studies. These compositional fluctuations are not present in the regions in between the columnar grains.
2. Annealing the Ag–40Cu film at 200 °C for 3 h leads to a progression of the phase-separation process via a

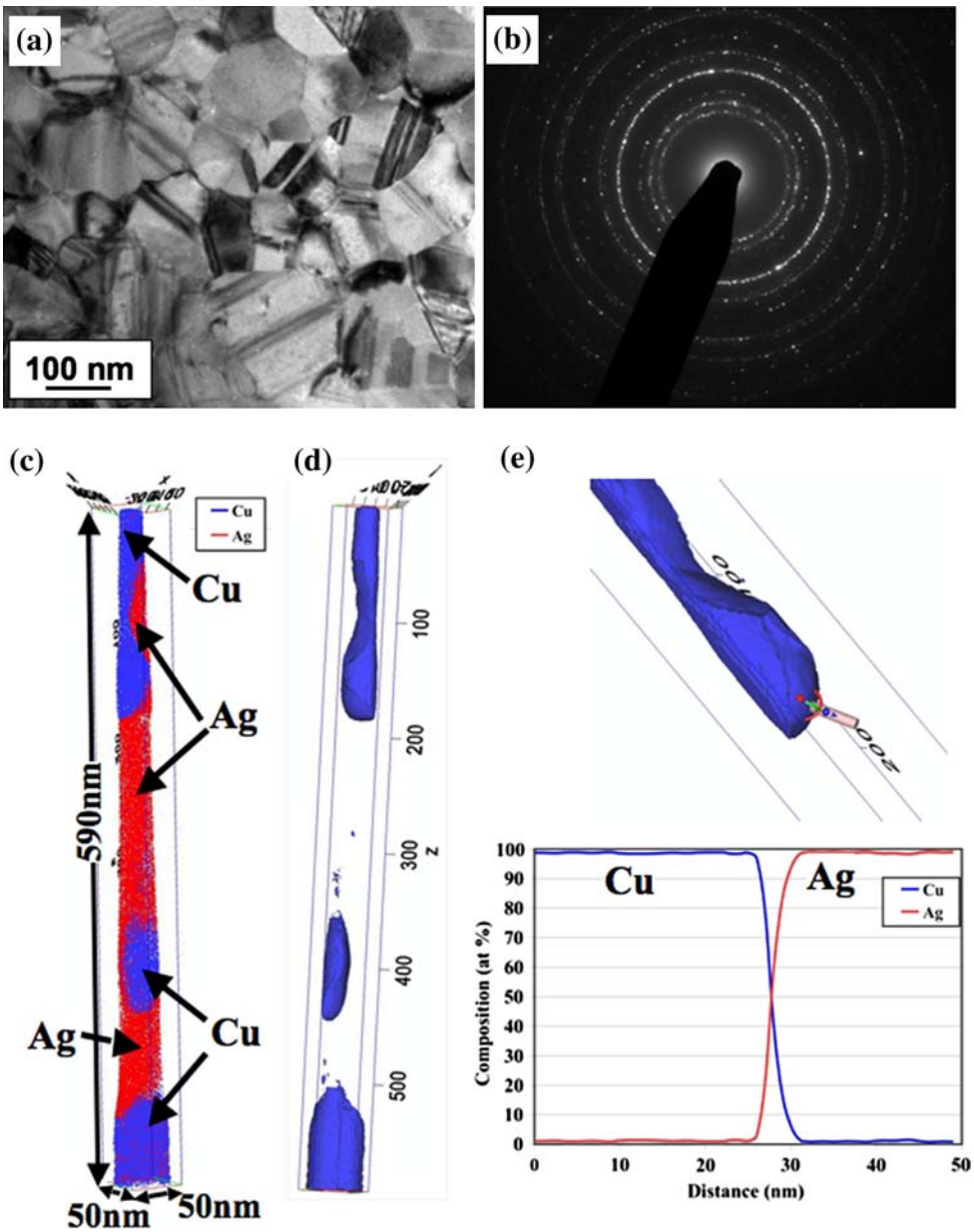

Fig. 6 (Color online) **a** Plan-view bright-field TEM image of 390 °C/24 h annealed Ag–40Cu film. **b** Corresponding selected area electron diffraction (SAD) pattern. **c** A 50 nm × 50 nm × 590 nm 3DAP reconstruction of 390 °C/24 h annealed Ag–40Cu film showing Cu atoms (in blue) and Ag atoms (in red). **d** A 50 at.% Cu iso-concentration surface from the same reconstruction showing the Cu-rich regions. **e** Magnified view of the Cu-rich region within this 3DAP reconstruction probed by a composition cylinder of 3-nm diameter, along with a corresponding composition profile

two-step mechanism. Initially, the compositional fluctuations present within the columnar grains become more pronounced and develop into longer-range periodic modulations with an average wavelength ~4 nm. This leads to a nanoscale-layered morphology within the columnar grains. Subsequently, recrystallization is initiated in the columnar grains leading to the formation of new equiaxed grains of *fcc* Cu (~97 at.% Cu), accompanied by the breakdown of the nanolayered structure within the columnar grains and eventually the columnar grains themselves.

3. Subsequent annealing at an even higher temperature of 390 °C for an extended time period of 24 h results in complete decomposition of the film into *fcc* Cu and *fcc* Ag grains. This is evident from both TEM diffraction and 3D atom probe results. Therefore, it can be concluded that the phase separation process has been completed in this case resulting in the formation of the thermodynamic equilibrium phases of *fcc* Cu and *fcc* Ag (~100 at.% Cu and ~100 at.% Ag).

References

1. Ma E (2005) Prog Mater Sci 50:413
2. Murray JL (1984) Metall Trans 15A:261
3. Alloy Phase Diagrams, ASM handbook, vol 3. ASM International (1992), p 238

4. Sheng HW, Wilde G, Ma E (2002) Acta Mater 50:475
5. He JH, Sheng HW, Lin JS, Schilling PJ, Tittsworth RC, Ma E (2002) Phys Rev Lett 89:125507
6. Duwez P, Willens RH, Klement WJ (1960) J Appl Phys 31:1136
7. Uenishi K, Kobayashi KF, Ishihara KN, Shingu PH (1991) Mater Sci Eng A 134:1342
8. Kazakos AM, Fahnline DE, Messier R, Pilione LJ (1992) J Vac Sci Technol A 10:3445
9. Huang YP, Yang Y, Chen Z et al (2008) J Mater Sci 43(15):5390. doi:10.1007/s10853-008-2793-9
10. Radiguet B, Etienne A, Pareige P et al (2008) J Mater Sci 43(23–24):7338. doi:10.1007/s10853-008-2875-8
11. Caballero FG, Miller MK, Garcia-Mateo C (2008) J Mater Sci 43(11):3769. doi:10.1007/s10853-007-2157-x
12. Capdevila C, Miller MK, Russell KF (2008) J Mater Sci 43(11):3889. doi:10.1007/s10853-007-2228-z
13. Gohil S, Banerjee R, Bose S, Ayyub P (2008) Scripta Mater 58(10):842
14. Barber ZH (1990) Vacuum 41:1102
15. Saunders N, Miodownik AP (1987) J Mater Sci 22:629. doi:10.1007/BF01160780629-637
16. Pagh Almtoft K, Ejsing AM, Bottiger J, Chevallier J, Schell N, Martins RMS (2007) J Mater Res 22:1018
17. Puthucode A, Kaufman MJ, Banerjee R (2008) Metall Mater Trans A 39(7):1578